Local and Global Dynamics during the Folding of *Escherichia coli* Dihydrofolate Reductase by Time-Resolved Fluorescence Spectroscopy†

Bryan E. Jones,‡,§ Joseph M. Beechem,*,|| and C. Robert Matthews*,‡

Department of Chemistry, Biotechnology Institute and Center for Biomolecular Structure and Function, The Pennsylvania State University, University Park, Pennsylvania 16802, and Department of Molecular Physiology and Biophysics, Vanderbilt University, Nashville, Tennessee 37232

Received August 17, 1994; Revised Manuscript Received December 5, 1994⊗

ABSTRACT: Time-resolved fluorescence techniques were utilized to monitor the kinetic refolding reaction of *Escherichia coli* dihydrofolate reductase (DHFR). Measurements of emission and anisotropy decay lifetimes of both the five intrinsic tryptophan residues and the fluorescent probe 1-anilinonaphthalene-8-sulfonate (ANS) during the folding reaction were used to characterize the compactness and development of tertiary structure in transient intermediates formed during the folding of DHFR. Experiments monitoring bound ANS show that a rapidly-formed intermediate (<20 ms) has a rotational time of ~10 ns and, therefore, a compactness similar to that for the native conformation. All of the tryptophan residues in this burst phase species rotate as freely as in the unfolded state. In the set of four intermediates which then appear over the next few hundred milliseconds, the apparent rotational time measured by ANS fluorescence increases to a maximum rotational time of ~20 ns. An increase in the average tryptophan lifetime for these intermediates suggests these side chains become excluded from solvent and associated dynamic quenching mechanisms. As the folding reaction proceeds to a set of four native conformers, the bound ANS rotational time then decreases to approach that for the native protein, 10.5 ns, and the average tryptophan rotational time increases to the same value. During these rate-limiting, final steps in folding, the static quenching effects which reflect the formation of specific tertiary contacts involving tryptophans also appear.

The formation of secondary structure and the development of nonpolar surfaces are important early events in the folding reactions of a variety of globular proteins. Because isolated fragments of proteins corresponding to elements of secondary structure are usually unfolded (Shin *et al.*, 1993; Lumb *et al.*, 1994), it is likely that the association of these elements stabilizes hydrogen bonding patterns (Kuwajima *et al.*, 1987; Sugawara *et al.*, 1991; Briggs & Roder, 1992; Jennings & Wright, 1993) and produces the surfaces to which hydrophobic dyes can bind (Ptitsyn *et al.*, 1990; Semisotnov *et al.*, 1991; Mann & Matthews, 1993; Itzhaki *et al.*, 1994; Jones *et al.*, 1994). This presumed intramolecular association reaction implies that the polypeptide condenses significantly in the first few milliseconds of folding; however, there have been few measurements of the compactness of proteins during folding reactions.

Electron spin resonance measurements on the folding of carbonic anhydrase B suggest that a compact species forms within 30 ms (Semisotnov *et al.*, 1987). Tryptophan fluorescence experiments of the folding of cytochrome *c* show an increase in fluorescence quenching by the heme in a rapidly formed intermediate (Elöve *et al.*, 1992). These data suggest that the burst phase intermediate is smaller than the unfolded state; however, a quantitative measurement of the size could not be made. Small-angle X-ray scattering has been used to monitor the evolution of the size during the refolding of apomyoglobin (Eliezer *et al.*, 1993). Unfortunately, the relatively high protein concentrations required to obtain usable signal/noise ratios in the millisecond time range appear to cause the dimerization of apomyoglobin during the refolding reaction. Dilatometry measurements indicate that ribonuclease A experiences a change in volume during folding; however, the 1−2 min dead time precludes the observation of rapid folding events (Ybe & Kahn, 1994).

A potential solution to this problem is offered by time-resolved spectroscopy of either intrinsic tryptophan fluorescence or the fluorescence of an extrinsic dye such as 1-anilinonaphthalene-8-sulfonate (ANS)[1] during protein folding reactions. Tryptophan fluorescence provides a measure of the local dynamics of these specific side chains while the fluorescence from bound ANS can offer insight into global dynamics. The lifetimes of the emission and the anisotropy of these fluorophores can be related to their environments and to their rotational relaxation times. Because there is typically a large difference in these parameters between the unfolded and native states of a protein, these techniques may be sensitive to the presence of partially folded structures (Eftink, 1994). Fluorescence spectroscopy has the additional advantage over light scattering of allowing the use of lower protein concentrations and, thereby, decreasing the possibility of aggregation.

† This work was supported by a grant from the NSF (MCB 9317273) to C.R.M. and by a grant from the NIH (GM 45990) and the Lucille P. Markey Foundation to J.M.B.

* Correspondence on fluorescence spectroscopy should be addressed to J.M.B. and correspondence on protein folding to C.R.M.

‡ The Pennsylvania State University.

§ Current address: Department of Biochemistry, University of Washington, Seattle, WA 98185.

|| Vanderbilt University.

⊗ Abstract published in *Advance ACS Abstracts,* February 1, 1995.

[1] Abbreviations: ANS, 1-anilinonaphthalene-8-sulfonate; CD, circular dichroism; DHFR, dihydrofolate reductase from *Escherichia coli*; K_2EDTA, ethylenediaminetetraacetic acid, dipotassium salt; MTX, methotrexate.

0006-2960/95/0434-1867$09.00/0

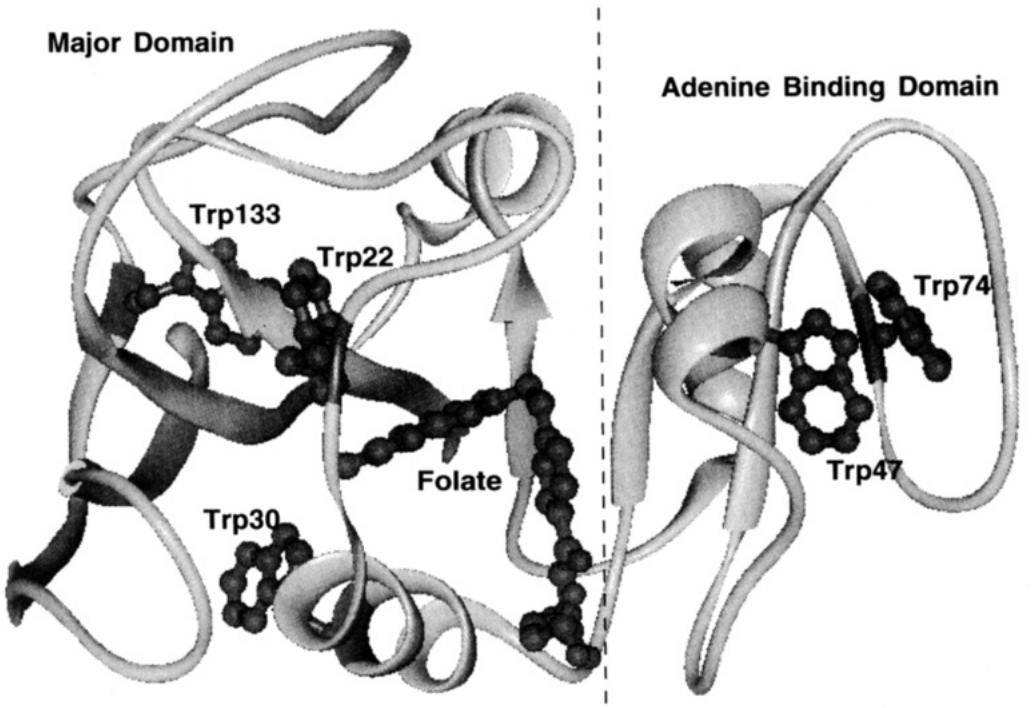

FIGURE 1: Ribbon diagram of the backbone of *E. coli* DHFR taken from the X-ray coordinates of the folate/$NADP^+$ ternary complex (Bystroff *et al.*, 1990). The five tryptophan residues are portrayed as are the adenine binding domain and the major domain. The fully oxidized form of the substrate, folate, is also shown to indicate the position of the substrate binding site.

Dihydrofolate reductase (DHFR) from *Escherichia coli* is an excellent candidate for such a time-resolved fluorescence study. The folding mechanism (Touchette *et al.*, 1986; Jennings *et al.*, 1993) is postulated to proceed initially through a species which appears within 5 ms, has significant secondary structure (Kuwajima *et al.*, 1991), binds ANS (Jones *et al.*, 1994), and has little stability. The emission intensity from the five tryptophan residues (Figure 1) in this burst phase intermediate is identical to that of the unfolded protein (Garvey *et al.*, 1989). This species then folds over several hundred milliseconds to a set of four intermediates, I_1-I_4, which also bind ANS, have Trp47 and Trp74 packed together in a native-like fashion, and have greater stability (Jones *et al.*, 1994). These intermediates finally fold to a corresponding set of native conformers, N_1-N_4, through four, parallel rate-limiting steps which require from 1−150 s at pH 7.8 and 15 °C. The sensitivity of the emission intensity of the tryptophans and the bound ANS to one or both of the early steps in the folding of DHFR suggests that these fluorophores could serve as useful probes of dynamic behavior in the millisecond time range.

In the present study, both total fluorescence intensity and anisotropy data (with full picosecond−nanosecond decay curves) were collected on the millisecond time-scale during the folding of DHFR. Full time-resolved decays permit one to examine the mechanism(s) associated with the changes in fluorescence properties which are observed during the actual folding reaction. The lifetime effects on the anisotropy function can also be explicitly taken into account. These measurements are, to our knowledge, the first experiments to provide millisecond timing resolution and anisotropy information. The total intensity class of "double-kinetic" experiments, with seconds−minutes time resolution, was first performed in the Brand laboratory (Walbridge *et al.*, 1987; Han *et al.*, 1987).

These time-resolved fluorescence techniques demonstrate that DHFR achieves a native-like compactness within 10 ms; however, the development of specific tertiary structure in the vicinity of the tryptophan residues can require many seconds. Surprisingly, the rotational relaxation time of bound ANS appears to increase to approximately double the initial value of 10 ns after 200 ms before returning to this value at the end of the folding reaction. This phenomenon does not appear to reflect aggregation of the protein.

EXPERIMENTAL METHODS

Reagents. Ultra-pure urea was purchased from ICN (Irvine, CA) and used without further purification. All other reagents were of reagent grade or better. The MTX affinity and DEAE-Sepharose resins used for protein purification were purchased from Sigma (St. Louis, MO) and Pharmacia (Piscataway, NJ), respectively. ANS was purchased from Molecular Probes (Eugene, OR). The concentration of ANS was determined by absorbance using $\epsilon_{370} = 6800\ M^{-1}\ cm^{-1}$ in methanol (Molecular Probes).

All folding experiments were carried out at 15 °C in a 10 mM potassium phosphate buffer (pH 7.80) containing 0.2 mM K_2EDTA and 1 mM β-mercaptoethanol.

Protein Purification. Purification of DHFR was performed as previously described (Jennings *et al.*, 1993). All purifications yielded material that migrated as a single band on sodium dodecyl sulfate−polyacrylamide gels (Laemmli, 1970). The specific activity ranged from 75 to 100 units mg^{-1} using the method of Hillcoat (Hillcoat *et al.*, 1967); the reported activity under these conditions is 85 units mg^{-1}. Protein concentration was determined by absorbance spectroscopy, using $\epsilon_{280} = 3.11 \times 10^4\ M^{-1}\ cm^{-1}$ (Touchette *et al.*, 1986).

Time-Resolved Fluorescence Measurements. Time-resolved fluorescence measurements at equilibrium were

performed with a Coherent Antares Nd:YAG laser (Palo Alto, CA). The output of this laser was frequency-doubled and used to synchronously pump a dual dye jet (Coherent 702) laser using rhodamine 6G for tryptophan excitation at 295 nm and kiton red for ANS excitation at 330 nm. Output pulses from the dye laser were utilized at 4 MHz and had a pulse width of approximately 1 ps. Time-resolved detection utilized time-correlated single-photon counting with a 6u Hamamatsu (R2809U-01, Bridgewater, NJ) microchannel plate detector, high-frequency 50× amplifiers (Phillips Scientific 774, Mahwah, NJ), constant fraction discriminators (Tennelec 454, Oak Ridge, TN), time-to-amplitude converters (Tennelec 862), and pulse-height analysis analog-to-digital converters (Nucleus PCA-II, Oak Ridge, TN). The instrument response was typically 40−80 ps. The collimated fluorescence emission was passed through a Hoya (Fremont, CA) 340 nm cuton filter for tryptophan or a Hoya 460 nm cuton filter for ANS emission and Glan-Thompson polarizers before being focused onto the entrance slit of a SPEX (Edison, NJ) 0.22 m emission monochromator. Tryptophan emission was measured at 350 nm, and ANS emission was measured at 470 nm. A half wave plate in the excitation beam was utilized to rotate the excitation polarization to horizontal for the determination of the polarization bias (g factor) of the detection instrumentation.

Double-Kinetic Measurements. Refolding reactions monitoring tryptophan fluorescence were performed with a Bio-Logic SFM-3 stopped-flow syringe system using a 1.5 mm × 1.5 mm fluorescence cuvette. Time-resolved data on the unfolded state were collected in the stopped-flow cuvette by 9-fold dilution of the 9 μM DHFR/5.4 M urea solution with 5.4 M urea using the stopped-flow drive train. This preshot mixture remained in the cuvette for 1 s prior to the initiation of the refolding reaction. Refolding was initiated by 9-fold dilution of the 9 μM DHFR/5.4 M urea solution with buffer to a final protein concentration of 1 μM at 0.6 M urea. The initiation of the syringe push was controlled by in-house software running on the computer that acquired the time-correlated emission data. Mixing artifacts which were presumed to be due to the use of only two syringes made it impossible to collect time-resolved tryptophan fluorescence data at times longer than ~5 s into the folding reaction.

Refolding experiments in the presence of ANS were carried out in a similar manner. Unfolded DHFR in 5.4 M urea was diluted 9-fold with buffer containing an appropriate concentration of ANS. Final protein concentrations ranged from 10 to 30 μM and final ANS concentrations from 10 to 15 μM. Because ANS is not observed to bind to the unfolded protein [this work and Jones *et al.* (1994)], an unfolded preshot was not used.

Excitation for the kinetic refolding experiments was identical to that for the static time-resolved measurements described above, with the exception that the excitation light was passed through a Glan-Thompson polarizer prior to the cuvette. For tryptophan fluorescence experiments, emission was detected as above, with the exception that the monochromator was not used. An analog TAC buffer pipeline circuit was utilized (Ying *et al.*, 1994) to increase the counting efficiency of photons detected in the double kinetic instrument. Although not absolutely necessary, this circuit board allowed for an additional 30% of the observed photons to be recorded. Photon counting rates were not exceptionally high, typically 30−50 kHz during the refolding reaction. For ANS fluorescence measurements, emission was detected similarly except that an additional in-house-designed ADC ping-pong circuit was employed (Ying, Piston, and Beechem, unpublished results). However, since the counting rates for the ANS experiments were only 5−10 kHz, the additional counting efficiency for this circuit was not completely utilized.

Time-resolved fluorescence data acquired during the refolding reaction were taken in discrete time slices of varying length. The start of the first time slice was correlated with the end of the syringe push that initiated the refolding reaction. The time slices during the reaction consisted 5 each of ~20, ~50, ~100, ~200, and ~500 ms. In addition, four time slices of 250 ms duration were taken during the time that the unfolded protein preshot mixture was in the cuvette. The true time for the center of each time slice after the initiation of the refolding reaction was calculated from the beginning and end of each time slice in reference to the internal clock of the computer.

The timing calibration for tryptophan fluorescence experiments was 12 ps/channel, and, typically, 2000−3000 channels of data were taken during each time slice. For ANS fluorescence measurements, the timing calibration was 24 ps/channel, and 900 channels of data were collected. The time-resolved data were summed over the duration of each time slice for each shot and stored. Typically, the emission polarizer orientation was changed every 25 shots, and a total of 600−1500 shots were collected per experiment in order to achieve sufficient signal-to-noise ratios for the time slices of shortest duration. Typical total intensity sum curves had approximately 4000−10 000 counts in the peak channel.

Total integrated intensity was recorded simultaneously with time-resolved data collection using a Hamamatsu R-928 photomultiplier tube mounted perpendicular to the excitation light. The photomultiplier tube was operated in the photon counting mode, with total counts being discriminated with a Stanford Research SR-400 discriminator and amplified with a Stanford Research SR455-DC300 amplifier. Total photons counted were recorded with a Tennelec Nucleus MCS-II multichannel scaler card and data collection software. Data acquired in this manner also served to confirm the true time points of the time slices obtained in relation to the initiation of the refolding reaction.

Data Analysis. Time-correlated fluorescence intensity decay data obtained for both horizontal (I_H) and vertical (I_V) polarizer orientations were used to calculate the total intensity [$S(t)$] and anisotropy decays [$r(t)$] with eqs 1 and 2:

$$S(t) = gI_V + 2I_H \quad (1)$$

$$r(t) = \frac{gI_V - I_H}{gI_V + 2I_H} \quad (2)$$

where g is the polarization bias of the detection instrumentation. Total intensity decays for both tryptophan and ANS fluorescence were well fit by two emission lifetimes, described by eq 3:

$$S(t) = \alpha_1 e^{-t/\tau_1} + \alpha_2 e^{-t/\tau_2} \quad (3)$$

where α_i is the amplitude of the emission lifetime τ_i. The tryptophan fluorescence anisotropy decays were well fit by

two rotational terms, described by eq 4:

$$r(t) = \beta_1 e^{-t/\phi_1} + \beta_2 e^{-t/\phi_2} \quad (4)$$

where ϕ_i represents the rotational correlation time with amplitude β_i. The initial anisotropy, r_0, is the sum of β_1 and β_2.

The time-resolved fluorescence anisotropy decay for ANS displays a completely associative behavior (Ludescher *et al.*, 1987). ANS bound to DHFR has a much longer emission lifetime (~10 ns) than free ANS (~0.15 ns); therefore, a simple associative modeling scheme was utilized for analysis of the ANS intensity decays for each emission polarization (Beechem *et al.*, 1991):

$$I_V = (1/3)\alpha_f e^{-t/\tau_f}[1 + 2\beta_f e^{-t/\phi_f}] + (1/3)\alpha_b e^{-t/\tau_b}[1 + 2\beta_b e^{-t/\phi_b}] \quad (5)$$

$$I_H = (1/3)\alpha_f e^{-t/\tau_f}[1 - \beta_f e^{-t/\phi_f}] + (1/3)\alpha_b e^{-t/\tau_b}[1 - \beta_b e^{-t/\phi_b}] \quad (6)$$

where the subscripts represent the free (f) and bound (b) states of ANS. The time-resolved total intensity [$S(t)$] and anisotropy [$r(t)$] decays were then calculated as above (eqs 1 and 2). Both the free and bound states of ANS were very well approximated with only a single lifetime and single rotational time each.

The time-correlated emission and anisotropy parameters were obtained by simultaneous analysis of the intensity decays for both emission polarizer orientations using the GLOBALS UNLIMITED software package (Beechem *et al.*, 1991). Results of double kinetic experiments as a function of folding time were fit to a sum of exponentials using NLIN (SAS Institutes, Cary, NC) running on either a Swan 386/25 personal computer or an IBM RS 6000 workstation.

RESULTS

Steady-state fluorescence stopped-flow studies have proven extremely useful for characterizing changes in populations associated with intermediate states in a variety of protein folding reactions [see, for example, Touchette *et al.* (1986) and Elöve *et al.* (1992)]. Unfortunately, the information content of the steady-state fluorescence signal is rather limited. The steady-state signal change represents an integral over the time-resolved fluorescence decay function, and, therefore, cannot provide information regarding the underlying photophysical mechanism associated with the observed change in intensity. Experiments which record the stopped-flow steady-state fluorescence anisotropy can provide important additional information (Otto *et al.*, 1994) but still represent a time-averaged integral quantity.

The detection of time-correlated fluorescence emission during the folding of DHFR is similar to standard time-resolved spectroscopy, with the exception that data collection is divided into small time slices, ranging in duration from 20 ms for the early times in folding to 1 s at longer times. The low signal-to-noise resulting from this short detection period was improved by averaging 300−750 refolding runs for each emission polarizer orientation. Representative total intensity and anisotropy decay curves for both tryptophan and ANS fluorescence during the refolding reaction are shown in Figures 2 and 3, respectively.

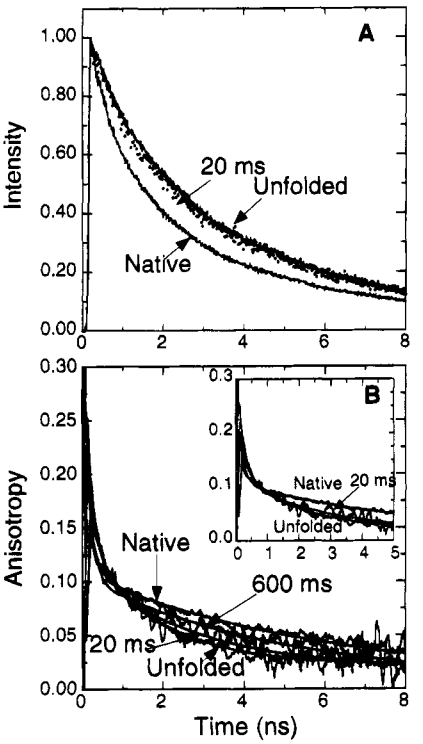

FIGURE 2: Time-resolved tryptophan fluorescence total intensity and anisotropy decays. (A) Total intensity traces shown are for the unfolded preshot (500 ms time slice), the first time slice at 20 ms (20 ms duration), and the native protein in 0.6 M urea. The initial increase reflects the initial response to the laser pulse. (B) Anisotropy decays shown are for the unfolded preshot (500 ms time slice), the first time slice at 20 ms (20 ms duration), a time slice taken at 600 ms (50 ms duration), and the native protein in 0.6 M urea. The inset shows decays for the native, unfolded, and first time slice. Solid lines are fits obtained from analysis with the GLOBALS software (Beechem *et al.*, 1991). The data for time slices during the refolding reaction represent the average of 600 shots (300 for each emission polarizer orientation).

The total tryptophan intensity decay obtained from the first time slice during the refolding reaction at 0.6 M urea (20 ms in duration centered at 20 ms after initiation of refolding) is compared to the intensity decay of native protein in 0.6 M urea and that for the unfolded protein (DHFR in 5.4 M urea; taken from a 250 ms time slice during the unfolded preshot) in Figure 2A. The total intensity decay curves for the unfolded protein and the first time slice are virtually superimposable, indicating that the tryptophan emission properties are essentially identical to those of the unfolded protein after the first 20 ms of folding. This result is consistent with previous results (Garvey *et al.*, 1989) which demonstrated that no changes in tryptophan fluorescence intensity occur within the dead time of stopped-flow experiments, 5 ms. As folding progresses, the decay curves approach that of the native protein.

A similar effect is observed in the tryptophan anisotropy decay curves (Figure 2B). The curve obtained from the first time slice is nearly superimposable with the anisotropy decay curve for the unfolded protein. The decay curves then progress monotonically toward that observed for the native protein as folding continues. These measurements show that the environments and rotational properties of the tryptophan side chains are essentially identical both in the unfolded protein and in the first, rapidly formed folding intermediate for DHFR.

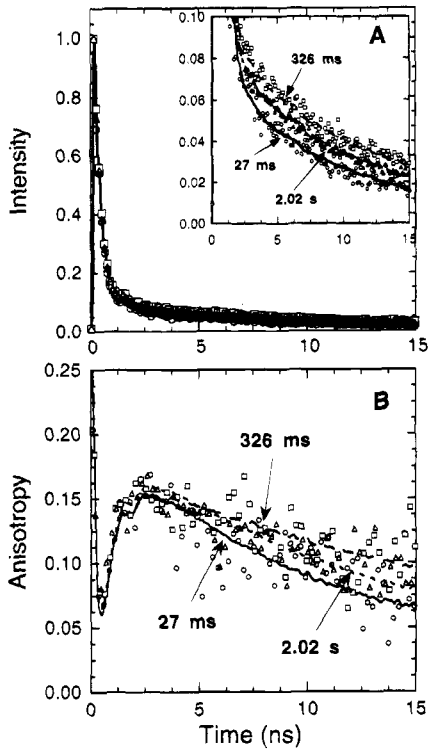

FIGURE 3: Time-resolved ANS fluorescence total intensity and anisotropy decays. (A) Total intensity decays are shown for time slices centered at 27 ms (10 ms in duration; circles), 326 ms (100 ms in duration; squares), and 2.02 s (200 ms in duration; triangles) during the refolding reaction. The inset shows changes in the long lifetime emission of ANS during the refolding reaction. The initial increase reflects the initial response to the laser pulse. (B) Corresponding anisotropy decays for the same time slices. Lines indicate fits of the data obtained from analysis with the GLOBALS software (Beechem *et al.*, 1991). The refolding reaction was initiated by a 9-fold dilution of DHFR with buffer containing ANS at 15 °C. The final protein concentration was 30 μM, and the ANS concentration was 15 μM.

Total intensity and anisotropy decays for ANS bound to DHFR during the folding reaction are shown in Figure 3. Evident in the total intensity decays are two well-separated emission lifetimes. The larger amplitude decay occurs in hundreds of picoseconds, and the smaller amplitude, longer lifetime emission occurs in tens of nanoseconds. Experiments with free ANS reveal that the short emission lifetime is due to free ANS in solution (data not shown), implying that the longer lifetime is associated with ANS bound to DHFR. As can be seen in the inset of Figure 3A, nonmonotonic changes in the long lifetime emission occur during the folding reaction. Note that because ANS does not bind to unfolded DHFR (Jones *et al.*, 1994), the signals which reflect bound ANS reflect the presence of folding intermediates.

The distinct time-resolved characteristics of free and bound ANS provide complete discrimination of the picosecond–nanosecond decay data obtained on the millisecond timescale. Steady-state versions of this experiment would be dominated by the large amount of free dye which is always present during refolding, due to the relatively low affinity of ANS for DHFR. It is evident that the photophysical mechanism associated with the change in ANS fluorescence involves both static and dynamic quenching components, as both lifetimes and amplitudes smoothly change throughout these reaction phases (see discussion below).

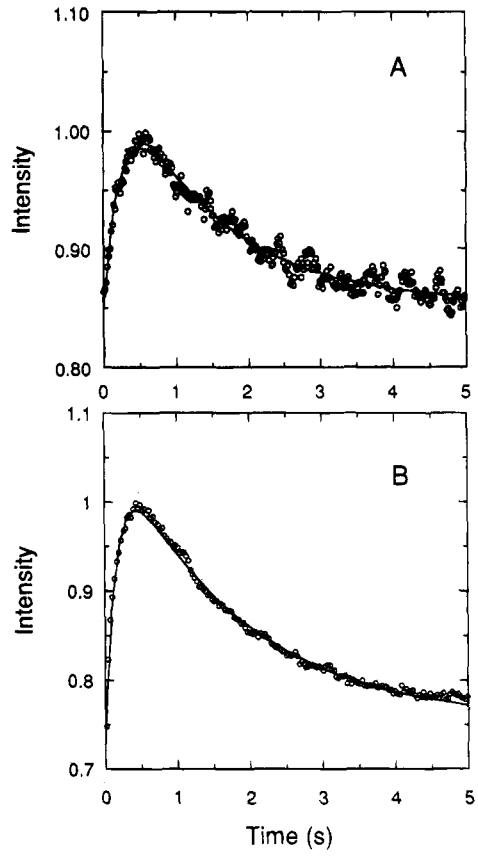

FIGURE 4: Integrated tryptophan (A) and ANS (B) fluorescence intensity traces for the refolding of DHFR measured simultaneously with time-resolved data collection. The conditions for tryptophan fluorescence were as described in the legend of Figure 2. ANS intensity at 30 μM DHFR and 15 μM ANS was measured as described in the legend of Figure 3. Solid lines are nonlinear least-squares fits of the data to a sum of two exponentials.

The anisotropy decays associated with the total intensity decays for ANS fluorescence are shown in Figure 3B. The complex dependence, compared to the simpler, exponential decay exhibited by the tryptophan fluorescence, is characteristic of an associative process (Ludescher *et al.*, 1987). In this case, the two, well-separated anisotropy decays are associated with the two emission lifetimes. The faster anisotropy decay occurs during the emission by free ANS, and the longer anisotropy decay occurs during the emission of ANS bound to the protein. As can be seen in Figure 3B, the duration of the long anisotropy decay for ANS also varies nonmonotonically during the folding reaction.

Total Integrated Intensity. To ensure that the double kinetic instrument was performing properly, a standard photomultiplier tube was mounted perpendicular to the excitation light from the laser in order to monitor the total emission intensity during the refolding reaction simultaneously with the time-resolved data collection. The intensity for tryptophan emission obtained in this manner shows an increase within the first 500 ms before decreasing at longer times (Figure 4A). This rise in intensity has been shown to reflect the burial of Trp74 within a hydrophobic cluster during this phase (Garvey *et al.*, 1989). The nonlinear least-squares fit of these data to two exponentials yielded relaxation times of 0.25 ± 0.01 and 1.05 ± 0.09 s (Table 1), values which are very similar to those previously observed for the $\tau_5$and τ_4 refolding phases, respectively (Touchette *et al.*, 1986; Kuwajima *et al.*, 1991; Jennings *et al.*, 1993).

Table 1: Relaxation Times and Amplitudes from Fits of Fluorescence Intensities, Emission Properties, and Rotational Properties during Refolding

fluorophore	parameter	τ_{fast} (s)	A_{fast}	τ_{slow} (s)	A_{slow}
Trp	int. int.[a]	0.25 ± 0.01	−0.27 ± 0.01	1.05 ± 0.09	0.232 ± 0.009
ANS, 10 μM DHFR	int. int.	0.211 ± 0.002	−0.305 ± 0.002	1.36 ± 0.01	0.267 ± 0.002
ANS, 30 μM DHFR	int. int.	0.214 ± 0.001	−0.385 ± 0.002	1.37 ± 0.01	0.337 ± 0.001
Trp	τ_L[b]	0.31 ± 0.07	−0.96 ± 0.08	1.2 ± 0.8	0.20 ± 0.07
Trp	α_L[c]	ND	ND	1.5 ± 0.5	0.49 ± 0.01
ANS	τ_L	0.14 ± 0.04	−2.3 ± 0.3	1.7 ± 0.3	2.0 ± 0.2
ANS, 10 μM DHFR	α_L	0.3 ± 0.2	−0.013 ± 0.006	1.6 ± 0.8	0.008 ± 0.001
ANS, 30 μM DHFR	α_L	0.3 ± 0.1	−0.03 ± 0.01	1.7 ± 0.4	0.02 ± 0.01
Trp	ϕ_L[d]	ND	ND	1.4 ± 0.6	−1.4 ± 0.3
Trp	r_0[e]	0.18 ± 0.04	0.052 ± 0.007	ND	ND
Trp	$<r>$[f]	0.2 ± 0.1	−0.008 ± 0.003	>2	<0.01
ANS, 10 μM DHFR	ϕ_L	0.06 ± 0.02	−14 ± 3	0.7 ± 0.2	10 ± 2
ANS, 30 μM DHFR	ϕ_L	0.06 ± 0.01	−22 ± 2	0.7 ± 0.1	12 ± 1

[a] Integrated fluorescence intensity. [b] Long emission lifetime. [c] Fractional amplitude of long emission lifetime. [d] Long rotational correlation time. [e] Initial anisotropy. [f] Steady-state anisotropy.

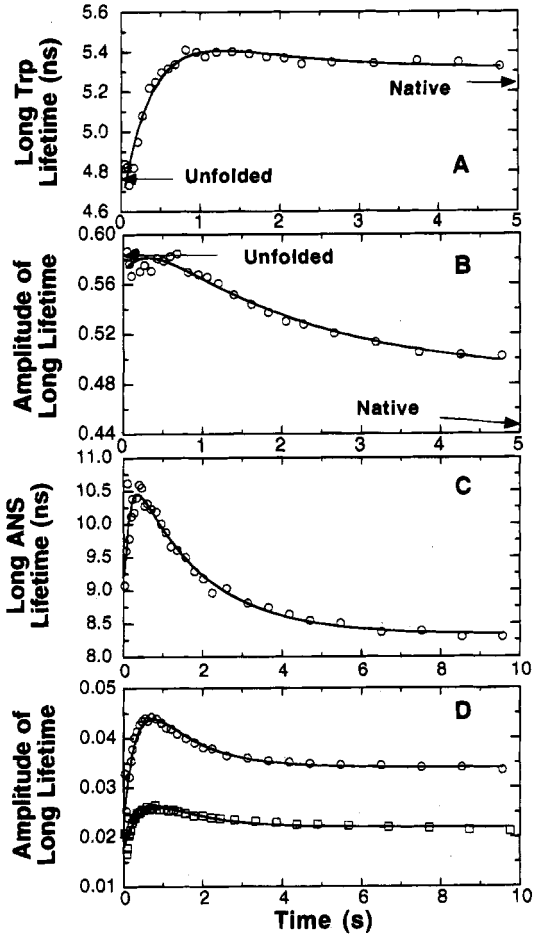

FIGURE 5: Plots of tryptophan and ANS fluorescence emission lifetimes and amplitudes during refolding. The long lifetime (A) and fractional amplitude (B) of the tryptophan emission were measured during the refolding of 1 μM DHFR at 0.6 M urea as described in Figure 2. The long lifetime (C) and fractional amplitude (D) for ANS emission were obtained from the refolding of 30 μM DHFR at 0.6 M urea in the presence of 15 μM ANS as described in Figure 3. Lines through the data indicate fits to a sum of exponentials whose parameters are shown in Table 1.

Similar results were obtained when monitoring ANS fluorescence during the folding reaction (Figure 4B). The rise and fall in intensity are identical to previous results obtained with another instrument (Jones *et al.*, 1994). Essentially identical relaxation times were observed at 30 μM DHFR and 15 μM ANS and at 10 μM DHFR and 10 μM ANS; only the amplitudes varied (Table 1). The relaxation times obtained from fits of these data are very similar to those obtained from tryptophan fluorescence (Figure 4A): 0.211 ± 0.002 and 1.36 ± 0.01 s at 10 μM DHFR, and 0.214 ± 0.001 and 1.37 ± 0.01 s at 30 μM DHFR (Table 1).

Total Intensity Emission Parameters. Analysis of the tryptophan total intensity decay curves obtained from the native and unfolded protein yielded two emission lifetimes, as did the decay curves obtained during the refolding reaction. The longer lifetime component, τ_L, is plotted versus folding time in Figure 5A. This lifetime increases from 4.72 ns, similar to the value of the unfolded protein, to ~5.4 ns at 1 s into the refolding reaction. The lifetime then decreases marginally over the remainder of the folding reaction. After 4.75 s, the value for this lifetime is 5.32 ns, within experimental error of that for the native protein, 5.28 ns. The shorter lifetime component appears to decrease from ~1.2 to ~1.1 ns over this same time range (data not shown). However, owing to the scatter in these data, the change is most likely insignificant.

The increase in the longer tryptophan lifetime component over the first second of the folding reaction correlates well with the increase in total intensity during the τ_5 folding phase (Figure 5A). When these data are fit to a sum of two exponentials, relaxation times of 0.31 ± 0.07 s for the increase and 1.2 ± 0.8 s for the decrease are obtained (Table 1). These values are within error of the relaxation times previously observed for the τ_5 and τ_4 folding phases by other methods (Touchette *et al.*, 1986; Jennings *et al.*, 1993) and those obtained from the fit of the total integrated intensity (Table 1).

The fractional amplitude of the longer lifetime, α_L, is plotted versus folding time in Figure 5B. The amplitude remains constant at ~0.58 for the first 500 ms, similar to the value observed for the unfolded protein. The magnitude then decreases exponentially to ~0.5 after 5 s. The value observed for the native protein, 0.44, is considerably smaller, indicating that substantial changes in this parameter occur during the slower refolding reactions. The lag phase observed here is similar to the lag phase observed when monitoring the binding of the inhibitor methotrexate to DHFR (Jennings *et al.*, 1993). This behavior indicates that the amplitude of this lifetime does not change during the formation of the intermediates by the τ_5 phase. These data

were fit to two exponentials, with the faster used to approximate the observed lag phase. The relaxation time obtained for the decrease in the amplitude of the long emission was 1.5 ± 0.5 s, within error of the above values for the τ_4 refolding reaction (Table 1).

These data unequivocally reveal that the photophysical mechanisms associated with the rising and falling phases of the tryptophan total intensity signal are different. The rising phase is associated with a change in the dynamic quenching properties of the tryptophans (i.e., changes in the photophysical environment which the tryptophan residues experience during the mean lifetime of the excited-state). During the rising phase of the steady-state intensity, the photophysical environment of the 4.7 ns tryptophan lifetime class (which may represent a complex average of the "long-lived" tryptophans in DHFR) changes to 5.4 ns. This 15% increase in tryptophan lifetime matches almost exactly the increase in steady-state fluorescence intensity which is observed (0.86 → 1.0; see Figure 4A). Therefore, the rising phase of the steady-state fluorescence signal is completely dynamic in character.

The long emission lifetime and its amplitude for ANS fluorescence are shown in Figure 5C and Figure 5D, respectively. In this case, both the intensity and amplitude increase and then decrease during the folding reaction. The relaxation times obtained for these changes in lifetime during refolding are 0.14 ± 0.04 and 1.7 ± 0.3 s (Table 1), similar to the values obtained from fits of the total intensity data shown in Figure 4B. The fractional amplitudes obtained from experiments at both 10 and 30 μM DHFR are shown in Figure 5D. Fits of these data yielded relaxation times of 0.3 ± 0.2 and 1.6 ± 0.8 s for the data obtained at μM DHFR and 0.3 ± 0.1 and 1.7 ± 0.4 s at 30 μM DHFR (Table 1). As with the total integrated intensity, only the magnitudes varied with the protein concentration (Table 1); the observed relaxation times were independent of protein concentration and are in excellent agreement.

Rotational Parameters. The parameters obtained from analysis of the tryptophan anisotropy decay curves for each time slice during the refolding of DHFR are shown in Figure 6. The time dependence of the long rotational correlation time, ϕ_L, is plotted in Figure 6A. As expected from inspection of the tryptophan anisotropy decays (Figure 2), the rotational correlation times for the unfolded protein and the first time slice for the refolding protein are similar. These values increase during the first 5 s of the refolding reaction from 4.5 ns to 6 ns. At ~5 s into the folding reaction, the value for the longer rotational correlation time has progressed only ~1/3 of the difference between the values observed for the unfolded and native protein. This increase in correlation time could be fit to a single exponential with a relaxation time of 1.4 ± 0.8 s (Table 1), similar to the τ_4 phase described above. As the protein continues to fold, the tryptophans become more tightly packed and begin to reflect the rotational properties of the entire protein.

The initial anisotropy, r_0, can be calculated from the sum of the amplitudes of the two rotational times and is plotted in Figure 6B. The change in this parameter from the unfolded to the native conformation appears to occur entirely within the first 1 s of the refolding reaction. This effect is also evident in the crossover of the anisotropy decays at ~0.5 ns (Figure 2B). The data can be fit well to a single exponential with a relaxation time of 0.18 ± 0.04 s (Table 1), similar to the relaxation time expected for the τ_5 refolding phase. The decrease in r_0 reflects the formation of a tryptophan−tryptophan eximer (Ge & Georghiou, 1991), which has previously been characterized by CD spectroscopy (Kuwajima *et al.*, 1991).

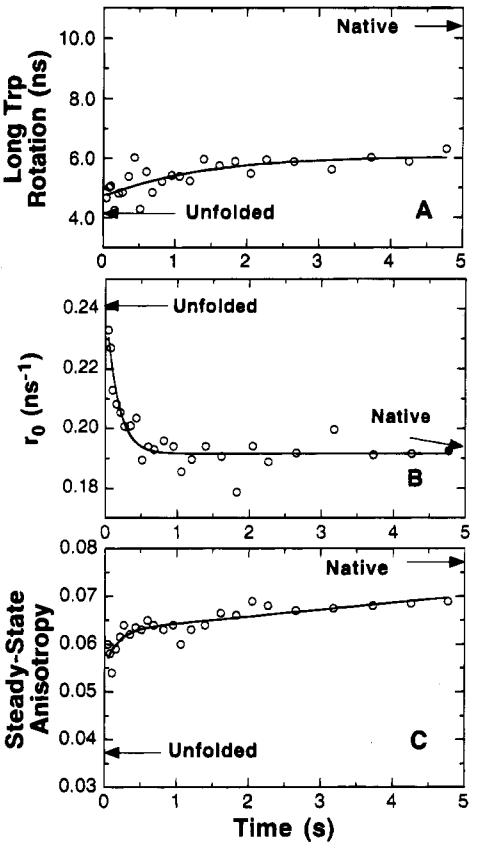

FIGURE 6: Plots of tryptophan rotational properties during the refolding reaction. The long rotational time (A), initial anisotropy (B), and steady-state anisotropy (C) for tryptophan emission were measured during the refolding of 1 μM DHFR at 0.6 M urea as described in Figure 2. Lines through the data indicate fits to a sum of exponentials whose parameters are shown in Table 1.

The steady-state anisotropy, $\langle r \rangle$, can also be calculated from the time-resolved data and can also serve as a useful monitor of protein folding reactions (Eftink, 1994). Preliminary experiments using a continuous light source to monitor the steady-state anisotropy during the refolding reaction revealed the presence of a large change occurring within the dead time of stopped-flow experiments, 5 ms (Jones, Beechem, and Matthews, unpublished results). This result appears to be in conflict with the observation that the time-resolved anisotropy decay curves for the unfolded protein and the first time slice are nearly identical. Therefore, the steady-state anisotropy was calculated from the time-resolved data by integration of the total counts for each time slice (Lakowicz, 1986). The steady-state anisotropy shows a jump from the unfolded value of 0.037 to ~0.055 within 10 ms of refolding (Figure 6C). As will be considered further in the Discussion, this jump is a result of a shift in the tryptophan absorbance spectra upon changing the urea concentration (Eftink, 1994).

Analysis of the anisotropy decay curves for each time slice revealed that the magnitude of the longer rotational relaxation time appears to vary during the folding reaction; the shorter relaxation time remains constant at ~0.15 ns (data not shown). The values of the longer relaxation time obtained

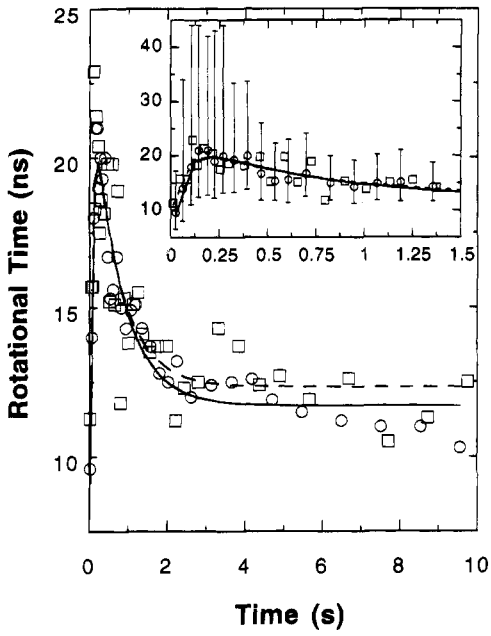

FIGURE 7: Long rotational time of bound ANS during the refolding reaction at 10 μM (squares) and 30 μM DHFR (circles). Fits of the data to a sum of two exponentials plus a constant are shown: 10 μM DHFR, dashed line; 30 μM DHFR, solid line. Standard, nonlinear errors are indicated by the symbol size. The error bars shown in the inset represent standard deviations of the recovered values determined by rigorous error analysis using GLOBALS, as described in the text. The inset shows the first 1.5 s of the reaction, with error bars shown only for the 30 μM DHFR data.

at both 10 μM and 30 μM DHFR are shown in Figure 7. Strikingly, the rotational time at ~20 ms into the folding reaction is very similar to that for ANS bound to the native protein (10.5 ns). During the first 200 ms, this value appears to increase to approximately 20 ns before decreasing to ~12 ns after 10 s into the refolding reaction. The magnitude of the errors in these calculations (Figure 7) suggests that this observation be considered tentative at this time. The longer rotational time estimated for fully folded DHFR, 10.5 ns, is within error of that obtained by tryptophan fluorescence (Figure 6A) and is consistent with that expected for a folded protein of this molecular mass (18 kDa; Cantor & Schimmel, 1980).

The observation that superimposable data are obtained at both 10 μM and 30 μM DHFR strongly suggests that the increase in rotational time occurring within the first 200 ms is not a result of protein aggregation. Fits of each data set yield nearly identical relaxation times for the increase in rotational time: 0.06 ± 0.02 s for 10 μM DHFR and 0.06 ± 0.01 s for 30 μM DHFR (Table 1). Although these values are somewhat smaller than those obtained by the other measurements (Table 1), the magnitude of the errors in the rotational relaxation times suggests that these differences are not significant. The identical behavior observed for the two different concentrations of DHFR also demonstrates the reproducibility of this effect.

DISCUSSION

ANS Dynamics during the Folding of DHFR. The measurement of fluorescence anisotropy decays of ANS bound to DHFR during folding provides insight into the dynamic behavior of the nonpolar surfaces to which it binds. Because the rotational relaxation time is proportional to the volume of the molecule (Cantor & Schimmel, 1980; Steiner, 1991), this parameter offers a measure of the compactness of a protein during the folding reaction. The identical rotational times observed for the native state by either tryptophan fluorescence or bound ANS fluorescence anisotropy decays, 10 ± 1 ns, and the excellent agreement of this value with that expected for a folded protein of this molecular mass (Cantor & Schimmel, 1980) show that ANS has the potential to provide an accurate probe of the size of the molecule during refolding.

Within 20 ms after the initiation of refolding, DHFR has a rotational relaxation time which is almost identical to that of the native state (Figure 7). This result could have two different structural interpretations. Either the burst phase intermediate has a compactness which is similar to that of the fully folded protein or the intermediate has subdomains which are capable of semi-independent motion. The formation of an extensive β-sheet detected by stopped-flow CD (Kuwajima *et al.*, 1991) and pulse-labeling NMR studies of amide hydrogen bonding (Jones & Matthews, 1995) favors the first explanation but does not rule out the second.

It has been proposed that a common early intermediate in protein folding involves the molten globule state, a compact species which has significant secondary structure, no specific tertiary structure, and marginal stability (Ptitsyn, 1987; Kuwajima, 1989). Stable models of molten globules have been obtained for a number of proteins, either at acidic pH with (Hamada *et al.*, 1993; Nishii *et al.*, 1994) or without (Kuwajima, 1989; Fink *et al.*, 1993) salt or at high temperature (Baum *et al.*, 1989). Viscosity and X-ray scattering studies suggest that these species have radii which are 10−20% (Dolgikh *et al.*, 1981, 1985; Nishii *et al.*, 1994) larger than those of the native conformations. Because the rotational relaxation times of polypeptides depend on their molecular volumes (Cantor & Schimmel, 1980; Steiner, 1991), the rotational relaxation times of molten globules would be predicted to be approximately 30−75% larger than those of the native conformations. The errors in the measurements of the rotational relaxation times are sufficiently large (Figure 7) that the burst phase intermediate for DHFR could satisfy this criterion for a molten globule.

Another striking observation is that the rotational time appears to increase to ~20 ns over the first 200 ms of refolding before decreasing to the value observation for the native conformation. The errors in these measurements are sufficiently large that this observation must be considered tentative. If the increase in rotational time is real, it implies an ~25% increase in the radius of the molecule if it remains spherical (Cantor & Schimmel, 1980; Steiner, 1991). This apparent increase in the radius could also reflect the coalescence of independent subdomains into a global structure which rotates more slowly. A third possibility is that as folding proceeds DHFR assumes an asymmetric shape, e.g., an ellipsoid, which could lead to slower tumbling around the long axis (Cantor & Schimmel, 1980; Steiner, 1991). The increase and subsequent decrease in the lifetime and amplitude of the longer ANS component (Figures 5C and 5D, respectively) in the same time range are another manifestation of this apparent nonmonotonic change in size and/or shape of DHFR during folding.

A standard, uncorrelated error analysis yields errors in the rotational times that are less than 10% of the measured values

(Figure 7). However, due to the limited lifetime of bound ANS (8−10 ns), the uncertainties in the recovered rotational times are expected to be asymmetric; larger errors are associated with longer correlation times. Rigorous error analysis was performed on these recovered results (at the 67% confidence limit; Beechem *et al.*, 1991), which are shown in the inset of Figure 7. Although the error limits are very large for both data sets, the good reproducibility of the data obtained at both protein concentrations strongly suggests that the increase and subsequent decrease in rotational time are real. The observation that the time dependence of the apparent increase in rotational relaxation time is independent of the protein concentration over the range from 10 to 30 μM (Figure 7) shows that this increase does not reflect transient aggregation of an initially monomeric species. The half-time of formation of a dimer should have decreased by 9-fold over this concentration range.

ANS Emission Properties. The characteristic rise and fall of ANS fluorescence intensity has been observed in studies of the folding of a number of proteins (Ptitsyn *et al.*, 1990; Semisotnov *et al.*, 1991; Jones *et al.*, 1994). The measurement of emission lifetimes sheds additional light on the properties of ANS when bound to various folding intermediates. The increase in integrated fluorescence intensity occurring over the first few hundreds of milliseconds of the folding reaction of DHFR (Figure 4B) appears to be a result of an increase in both the long emission lifetime and its fractional amplitude (Figure 5C,D).

The increase in lifetime (Figure 5C) is indicative of a decrease in dynamic quenching, presumably due to solvent, and is consistent with solvent accessibility measurements using water-soluble fluorescence quenchers (Jones *et al.*, 1994). The increase in fractional amplitude (Figure 5D) indicates that at this stage of folding, additional dye is bound. Together, these results suggest that, after initial binding to solvent-accessible nonpolar sites, ANS is sequestered into more solvent-excluded sites. A potential candidate for such sites is the interface between the two structural domains in DHFR, in the vicinity of the folate binding site (Figure 1).

The fractional amplitude for bound ANS, which directly reflects the fraction of fluorophores emitting with a particular lifetime (Lakowicz, 1986), represents only ~2−4% of the total ANS present in the refolding mixture. This observation is similar to that from a previous study (Chaffotte *et al.*, 1992) which estimated that only ~0.02 mol of ANS per mole of protein is bound to a truncated mutant of the β_2 subunit of tryptophan synthase. This mutant protein has characteristics which resemble those of folding intermediates for full-length proteins.

Although ANS only binds to a small fraction of the total protein population at any instant in time, changes in the long emission lifetime and its amplitude during the folding reaction follow the same time course as those detected by a number of other intrinsic spectroscopic probes (Table 1; Touchette *et al.*, 1986; Kuwajima *et al.*, 1991; Jennings *et al.*, 1993; Jones *et al.*, 1994). Also, the loss in the amplitude of the steady-state ANS intensity observed after 5 ms at increasing final urea concentrations in refolding (Jones *et al.*, 1994) is very similar to that observed for the far-UV CD signal (Kuwajima *et al.*, 1991). Because the latter signal is 40% that of the native conformation, it is clear that the ANS is not reflecting the behavior of a small fraction of the protein. Thus, ANS binds weakly to the folding intermediates in DHFR and provides an accurate, nonperturbing monitor of the folding reaction.

Tryptophan Dynamics during the Folding of DHFR. In contrast to the native state-like rotational dynamics displayed by ANS in the burst phase folding intermediate for DHFR, the tryptophan side chains are as mobile as in the unfolded protein (Figure 6A). This observation is consistent with the lack of effect on either the lifetime or the amplitude of the longer lifetime component of the tryptophan emission (Figure 5A and Figure 5B, respectively).

The apparent burst phase in the steady-state tryptophan anisotropy (Figure 6C) appears to contradict this conclusion. The resolution to this discrepancy is found by considering the effect of the shift in the tryptophan absorbance spectra to lower wavelengths caused by decreasing the urea concentration by 9-fold (Eftink, 1994). Because the excitation polarization spectrum also shifts, the excitation at 295 nm occurs at a point of higher intrinsic polarization for tryptophan (Valeur & Weber, 1971). This is purely a solvent effect and occurs instantaneously upon mixing, leading to the incorrect impression that the tryptophans are rotating more slowly. The absence of an effect on the rotational time in the burst phase (Figure 6A) is consistent with this interpretation.

As folding proceeds to the set of I_1−I_4 intermediates, the increase in emission lifetime (Figure 5A) suggests that one or more tryptophans are being buried in hydrophobic pockets which could retard solvent quenching mechanisms (Lakowicz, 1986). This conclusion is supported by previous results which demonstrated that Trp74 is buried in a solvent-excluded hydrophobic pocket (Garvey *et al.*, 1989) and that a native-like contact forms between Trp74 and Trp47 (Kuwajima *et al.*, 1991) in this same time range. The direct contact between these two tryptophans also explains the decrease in the initial anisotropy, r_0 (Figure 6B). Exciton formation in DNA has been shown to cause a similar depolarization (Ge & Georghiou, 1991). Because the total change in the r_0 value between the unfolded and native states occurs during this phase, this Trp47/Trp74 interaction must be native-like in the entire population of molecules. The same conclusion was reached in stopped-flow CD studies of DHFR (Kuwajima *et al.*, 1991). The absence of an effect on the amplitude of the longer lifetime component (Figure 5B) implies that static quenching mechanisms do not change in this step (Lakowicz, 1986). Note that the depolarization of the Trp47/Trp74 pair in this folding phase means that further changes in the depolarization in subsequent phases must reflect the behavior of one or more of the remaining tryptophans at positions 22, 30, and 133 (Figure 1).

The rate-limiting steps in folding which are known to lead to a set of four native or native-like conformers (Touchette *et al.*, 1986; Jennings *et al.*, 1993) lead to rather large decreases in the amplitude of the longer tryptophan emission lifetime (Figure 5B) and increases in the rotational relaxation time (Figure 6A). These same folding reactions have little effect on the magnitude of the emission lifetime (Figure 5A). These results imply that dynamic quenching mechanisms, e.g., collision with solvent, change little in the later stages of folding but that motions of the tryptophan side chains become increasingly constrained. Static quenching increases in concert with the enhanced packing found in the native conformers. The rotational behavior of all five tryptophans

in the set of native conformers reflects that of the protein as a whole.

Implications for the Folding Mechanism of DHFR. The measurements of time-resolved fluorescence parameters for both intrinsic tryptophan residues and bound ANS offer new insights into the earliest events in the folding of DHFR. Within 20 ms, the protein collapses to a form which is nearly as compact as the fully folded protein. Stopped-flow CD (Kuwajima *et al.*, 1991) and hydrogen exchange NMR (Jones & Matthews, 1994) data show that a substantial fraction of this species has a native-like β-sheet with the complex strand topology found in DHFR, +2x +1x +1x −3x −2x −2x + 1x. This species also binds ANS to nonpolar surfaces which remain relatively solvent-exposed (Jones *et al.*, 1994) and has its five tryptophan residues as mobile and solvent-exposed as in the unfolded protein.

Over the course of the next several hundred milliseconds, DHFR appears to evolve to a more tightly-linked structure or to an asymmetric shape (or both) as Trp47 and Trp74 assume a native-like packing and the hydrogen bonding network strengthens. These events occur during the τ_5 folding phase which has been postulated to correspond to the formation of the I_1-I_4 folding intermediates (Jennings *et al.*, 1993). Either structural explanation seems more probable for these species than an expanded sphere because pulse-labeling NMR studies (Jones & Matthews, 1995) have shown that the central β-sheet network has already formed and is stable. The putative asymmetry could reflect the formation of subdomains defined by clusters of nonpolar side chains. The simultaneous protection of the tryptophans from dynamic quenching mechanisms is consistent with the elimination of water as the hydrophobic contacts are made in such clusters. The observation that the exciton coupling between Trp47 and Trp74 in this intermediate has the same far-UV CD spectrum as that found in native DHFR (Kuwajima *et al.*, 1991) shows that these two side chains must maintain their relative distance and orientation in one of these clusters. In contrast, the rotational properties of the Trp22, Trp30, or Trp133 side chains indicate that these side chains are still very mobile. Taken together, these results could be interpreted to mean that portions of these putative hydrophobic clusters are solid-like and well-defined while others are liquid-like and not well-defined. Mutational analysis of a folding intermediate in barnase (Matouschek *et al.*, 1992) indicates that hydrophobic clusters may not form in a uniform fashion; some regions can be rather native-like while others are more unfolded-like.

The rate-limiting steps in folding correspond to the formation of a set of native or native-like species, N_1-N_4, via the $\tau_1-\tau_4$ reactions. The asymmetric shape diminishes, nonpolar binding sites for ANS become sequestered within the protein, and the remaining tryptophans adopt rigid environments. In terms of local dynamics, it is as if Trp22, Trp30, and Trp133 undergo a change in phase from liquid-like to solid-like at the final stage in folding (Jeng *et al.*, 1990).

Perhaps the most important general implication of these results is that the protein folding problem can be greatly simplified by the rapid collapse of the polypeptide to a compactness near that of the native conformation (Dill, 1985). Without the need to search all of the conformations available to a random coil (Levinthal, 1968), a protein may be able to search all of the accessible conformations on a biologically-feasible time scale (Zwanzig *et al.*, 1992; Sali *et al.*, 1994). With a few possible exceptions (Baker &Agard, 1994), the native conformation could then correspond to the global free energy minimum.

ACKNOWLEDGMENT

We thank Michael Otto for his assistance in setting up and performing preliminary experiments, and for numerous helpful comments and discussions.

REFERENCES

Baker, D., & Agard, D. A. (1994) *Biochemistry 33*, 7505−7509.
Baum, J., Dobson, C. M., Evans, P. A., & Hanley, C. (1989) *Biochemistry 28*, 7−13.
Beechem, J. M., Gratton, E., Ameloot, M., Knutson, J. R., & Brand, L. (1991) in *Topics in Fluorescence Spectroscopy: Principles*, II (Lakowicz, J. R., Ed.) pp 241−305, Plenum Press, New York.
Briggs, M. S., & Roder, H. (1992) *Proc. Natl. Acad. Sci. U.S.A. 89*, 2017−2021.
Bystroff, C., Oatley, S. J., & Kraut, J. (1990) *Biochemistry 29*, 3263−3277.
Cantor, C. R., & Schimmel, P. R. (1980) *Biophysical Chemistry*, Vol. V, pp 539−590, W. H. Freeman, New York.
Chaffotte, A. F., Cadieux, C., Guillou, Y., & Goldberg, M. E. (1992) *Biochemistry 31*, 4303−4308.
Dill, K. A. (1985) *Biochemistry 24*, 1501−1509.
Dolgikh, D. A., Gilmanshin, R. I., Brazhnikov, E. V., Bychkova, V. E., Semisotnov, G. V., Venyaminov, S. Y., & Ptitsyn, O. B. (1981) *FEBS Lett. 136*, 311−315.
Dolgikh, D. A., Abaturov, L. V., Bolotina, I. A., Braznikov, E. V., Bychova, V. E., Gilmanshin, R. I., Lebedev, Y. O., Semisotnov, G. V., Tiktopulo, E. I., & Ptitsyn, O. B. (1985) *Eur. Biophys. J. 13*, 109−121.
Eftink, M. (1991) in *Topics in Fluorescence Spectroscopy: Principles*, II (Lakowicz, J. R., Ed.) pp 53−126, Plenum Press, New York.
Eftink, M. R. (1994) *Biophys. J. 66*, 482−501.
Eliezer, D., Chiba, K., Tsuruta, H., Doniach, S., Hodgson, K. O., & Kihara, H. (1993) *Biophys. J. 65*, 912−917.
Elöve, G. A., Chaffotte, A. F., Roder, H., & Goldberg, M. E. (1992) *Biochemistry 31*, 6876−6883.
Fink, A. L., Calciano, L. J., Goto, Y., Nishimura, M., & Swedberg, S. A. (1993) *Protein Sci. 2*, 1155−1160.
Garvey, E. P., Swank, J., & Matthews, C. R. (1989) *Proteins: Struct., Funct., Genet. 6*, 259−266.
Ge, G., & Georghiou, S. (1991) *Photochem. Photobiol. 54*, 301−305.
Hamada, D., Hoshino, M., Kataoka, M., Fink, A. L., & Goto, Y. (1993) *Biochemistry 32*, 10351−10358.
Han, M. K., Walbridge, D. G., Knutson, J. R., Brand, L., & Roseman, S. (1987) *Anal. Biochem. 161*, 479−486.
Hillcoat, B. L., Nixon, P. F., & Blakely, R. L. (1967) *Anal. Biochem. 21*, 178−189.
Itzhaki, L. S., Evans, P. A., Dobson, C. M., & Radford, S. E. (1994) *Biochemistry 33*, 5212−5220.
Jeng, M.-F., Englander, S. W., Elove, G. A., Wand, A. J., & Roder, H. (1990) *Biochemistry 29*, 10433−10437.
Jennings, P. A., & Wright, P. E. (1993) *Science 262*, 892−896.
Jennings, P. A., Finn, B. E., Jones, B. E., & Matthews, C. R. (1993) *Biochemistry 32*, 3783−3789.
Jones, B. E., & Matthews, C. R. (1995) *Protein Sci.* (in press).
Jones, B. E., Jennings, P. A., Pierre, R. A., & Matthews, C. R. (1994) *Biochemistry 33*, 15250−15258.
Kuwajima, K. (1989) *Proteins: Struct., Funct., Genet. 6*, 87−103.
Kuwajima, K., Yamaya, H., Miwa, S., Sugai, S., & Nagamura, T. (1987) *FEBS Lett. 221*, 115−118.
Kuwajima, K., Garvey, E. P., Finn, B. E., Matthews, C. R., & Sugai, S. (1991) *Biochemistry 30*, 7693−7703.
Laemmli, U. K. (1970) *Nature 227*, 680−685.
Lakowicz, J. R. (1983) *Principles of Fluorescence Spectroscopy*, pp 112−185, Plenum Press, New York.

Levinthal, C. (1968) *J. Chim. Phys. 65*, 44−45.
Ludescher, R. D., Peting, L., Hudson, S., & Hudson, B. (1987) *Biophys. Chem. 28*, 59−75.
Lumb, K. J., Carr, C. M., & Kim, P. S. (1994) *Biochemistry 33*, 7361−7367.
Mann, C. J., & Matthews, C. R. (1993) *Biochemistry 32*, 5282−5290.
Matouschek, A., Serrano, L., & Fersht, A. R. (1992) *J. Mol. Biol. 224*, 819−835.
Nishii, I., Katoaka, M., Tokunaga, F., & Goto, Y. (1994) *Biochemistry 33*, 4903−4909.
Otto, M. R., Lillo, M. P., & Beechem, J. M. (1994) *Biophys. J. 67*, 2511−2521.
Ptitsyn, O. B. (1987) *J. Protein Chem. 6*, 273−293.
Ptitsyn, O. B., Pain, R. H., Semisotnov, G. V., Zerovnik, E., & Razgulyaev, O. I. (1990) *FEBS Lett. 262*, 20−24.
Sali, A., Shakhnovich, E., & Karplus, M. (1994) *Nature 369*, 248−251.
Semisotnov, G. V., Rodionova, N. A., Kutyshenko, V. P., Ebert, B., Blanck, J., & Ptitsyn, O. B. (1987) *FEBS Lett. 224*, 9−13.
Semisotnov, G. V., Rodionova, N. A., Razgulyaev, O. I., Uversky, V. N., Gripas, A. F., & Gilmanshin, R. I. (1991) *Biopolymers 31*, 119−128.
Shin, H.-C., Merutka, G., Waltho, J. P., Tennant, L. L., Dyson, H. J., & Wright, P. E. (1993) *Biochemistry 32*, 6356−6364.
Steiner, R. F. (1991) in *Fluorescence Spectroscopy: Principles*, II (Lakowicz, J. R., Ed.) pp 1−52, Plenum Press, New York.
Sugawara, T., Kuwajima, K., & Sugai, S. (1991) *Biochemistry 30*, 2698−2706.
Touchette, N. A., Perry, K. M., & Matthews, C. R. (1986) *Biochemistry 25*, 5445−5452.
Valeur, B., & Weber, G. (1977) *Photochem. Photobiol. 25*, 441−444.
Walbridge, D. G., Knutson, J. R., & Brand, L. (1987) *Anal. Biochem. 161*, 467−478.
Ybe, J. A., & Kahn, P. C. (1994) *Protein Sci. 3*, 638−649.
Ying, G. T., Piston, D. W., & Beechem, J. M. (1994) *Biophys. J. 66*, A161.
Zwanzig, R., Szabo, A., & Bagchi, B. (1992) *Proc. Natl. Acad. Sci. U.S.A. 89*, 20−22.

BI941896L